Capture from *n* = 2 states of hydrogen by heavy fast ions

1997 Phys. Scr. 56 279

(http://iopscience.iop.org/1402-4896/56/3/009)

Physica Scripta. Vol. 56, 279–283, 1997

Capture from $n = 2$ states of hydrogen by heavy fast ions

C. C. Montanari, M. S. Gravielle and J. E. Miraglia

Instituto de Astronomía y Física del Espacio, Consejo Nacional de Investigaciones Científicas y Técnicas. C.C. 67, Suc. 28, 1428 Buenos Aires, Argentina

Received July 2, 1996; accepted in revised form January 8, 1997

Abstract

Electron capture cross sections from excited states H(2s) and H(2p) by collisions with H^+, He^{2+} and Li^{3+} ions are calculated using the eikonal impulse and continuum-distorted-wave approximations at moderate and high impact velocities. Our results are compared with other theoretical methods. A scaling rule in terms of the projectile charge is presented for partial cross sections.

1. Introduction

Theoretical studies of charge transfer from the metastable state H(2s) by collisions with protons and other charged particles are needed for the interpretation of the physical phenomena occurring in the controlled fusion plasmas and astrophysical gases [1, 2]. Therefore, these collision systems have been investigated in the last years. In the low energy regime, the earliest theoretical works used the simple Landau-Zener approximation [3, 4] or the close-coupling method with molecular orbitals [5, 6]. At intermediate energies, two set of values can be mentioned: Classical Trajectory Monte Carlo (CTMC) results as reported by Blanco *et al.* [6], and recent close-coupling (CC) calculations using atomic states reported by Esry *et al.* [7] and Toshima and Lin [8]. At moderate and high energies, results obtained with the eikonal approximation were published by Chan and Eichler [9] but experimental data are not yet available. The aim of this work is to extend the study of capture from $H(n = 2)$ for energies higher than those considered in the previous reports. Atomic units are used.

We study the electron capture processes from H(2s) and H(2p) using the prior version of the eikonal impulse (EI) approximation. The impact velocity range considered corresponds to the intermediate ($Z_P \geqslant v \geqslant Z_T/n_i$) and high ($v > Z_P > Z_T/n_i$) energy regions, with Z_T (Z_P) being the target (projectile) charge, v the impact velocity, and $n_i = 2$ the principal quantum number of the initial state; the value $Z_T/n_i = 0.5$ a.u. corresponds to the initial electronic velocity. The EI approximation is a distorted wave method that makes use of the exact impulse wave function in the final channel and the eikonal wave function in the initial channel. The method has already proven to be successful in dealing with a variety of atomic collisions in which the target was initially in the ground state [10–12]. To compare with, we also calculate the continuum-distorted-wave (CDW) approximation. At intermediate energies, the trends of the EI and CDW results as the velocity decreases are compared with the CC values corresponding to the highest energy considered in Refs [7, 8].

The work is organized as follows. In Section 2.1, total capture cross sections by impinging of H^+ and He^{2+} projectiles are investigated. Partial capture cross sections to the $n = 4$ level of He^{2+} and Li^{3+} ions by collisions with H(2s) are presented in Section 2.2. In Section 3, we derive a scaling rule for the partial cross sections in terms of the projectile charge. Finally, in Section 4 we compare the asymptotic behavior of the first order (BK1) and the second order (BK2) Brinkman-Kramers approximation, and estimate the velocity where the double-collision mechanism becomes dominant.

The following definitions are used: $\sigma_{i,f}$ is the partial cross section corresponding to the transition from the initial state $i = n_i l_i m_i$ to the final state $f = n_f l_f m_f$, $\sigma_i = \Sigma_f \sigma_{i,f}$ is the total capture cross section from the initial state i, and $\sigma_{n_i} l_i = \Sigma_{m_i} \sigma_i/(2l_i + 1)$ is the total capture cross section from the $n_i l_i$ subshell. Details of the calculations of the EI and CDW approximations can be found in Refs [10] and [13], respectively.

2. Results

2.1. *Total capture cross sections*

We calculate the partial cross sections for capture from H(2s) and H(2p) to the final levels $n_f = 1 - 4$ of H^+ and He^{2+} ions. Total capture cross sections are obtained by employing an extrapolation rule for large n_f derived in Ref. [11].

Total capture cross sections from H(2s) by protons and alpha particles are shown in Figs 1(a) and 1(b), respectively. In both cases we compare the tendency of the EI results as the velocity is decreased with the CC calculations corresponding to the highest energies considered in Ref. [7]. These CC values are presumed to be the most reliable ones in the velocity range [0.1, 0.8] a.u. For proton impact, Fig.

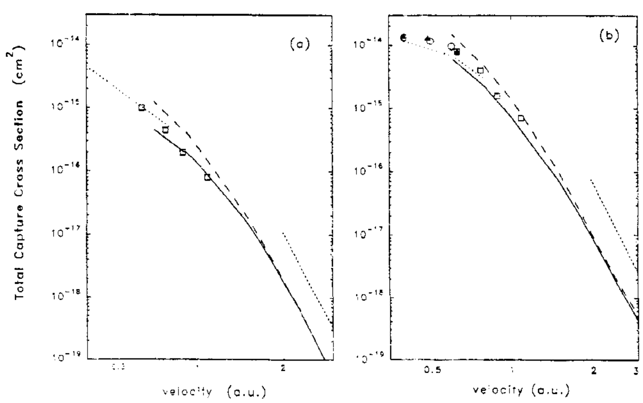

Fig. 1. Total capture cross section as a function of the impact velocity for protons (a) and alpha particles (b) colliding with H(2s). Solid line, EI results; long-dashed line, CDW results; short-dashed line, BK1 results; dotted line, CC calculations of Esry *et al.* [7]; hollow squares, results of Chan and Eichler [9]; filled triangles, results of Blanco *et al.* [6]; hollow circles, results of Jouin and Harel [14].

1(a), the EI curve seems to have the same slope as the CC calculations [7] but lying below them; while for alpha particles, Fig. 1(b), the EI results display good agreement with the CC values. In Fig. 1(b) we also show the CTMC results reported by Blanco *et al.* [6] and the molecular CC calculations of Jouin and Harel [14]. The eikonal results of Chan and Eichler [9] nicely connect the theoretical methods of high energies with those of intermediate energies. The eikonal approximation is supposed not to include the Thomas mechanism but this mechanism is only dominant at very high impact velocities, as studied in Section 4.

To check the performance of the EI theory we also calculate the CDW approximation. From Fig. 1 the CDW results converge to the EI curves as the velocity increases and run upon the CC values at intermediate energies. The BK1 cross sections are plotted only as reference at high energies with the aim of estimating the influence of multiple collision mechanisms. The large discrepancy between BK1 and EI (or CDW) approximations for $v > 2$ a.u. clearly suggests the importance of the double mechanism at high energies.

Total capture cross sections from H(2p) by collisions with protons and alpha particles are plotted in Figs 2(a) and 2(b), respectively. As in Fig. 1 we compare the behavior of the EI and CDW curves for intermediate velocities with the limit values of the CC calculations of Ref. [7]. The EI curves do not tend to the CC ones as the velocity decreases. The CDW values run upon the EI results for velocities lower than 1.5 a.u. and cross the CC curves. For proton projectiles the CDW and CC curves cross each other at $v \sim 0.8$ a.u. showing different slopes. At high energies EI and CDW results run together. Results for Li^{3+} projectiles are not displayed because there are no CC results available to compare with.

2.2. *Partial capture cross sections to* $n_f = 4$

In Figs 3 and 4 we plot partial cross sections corresponding to the level $n_f = 4$ for He^{2+} and Li^{3+} projectiles, respectively, impinging on H(2s). These contributions to individual $n_f l_f$ final states are of interest in astrophysical and thermonuclear plasma applications. The trends of the EI and CDW results as the velocities are decreased are compared with the CC calculations of Esry *et al.* [7] for He^{2+} and Toshima and Lin [8] for Li^{3+}. As in the previous subsection we also displayed BK1 results. For the sublevels 4s, 4p, and 4d the EI and CDW approximations present kinks,

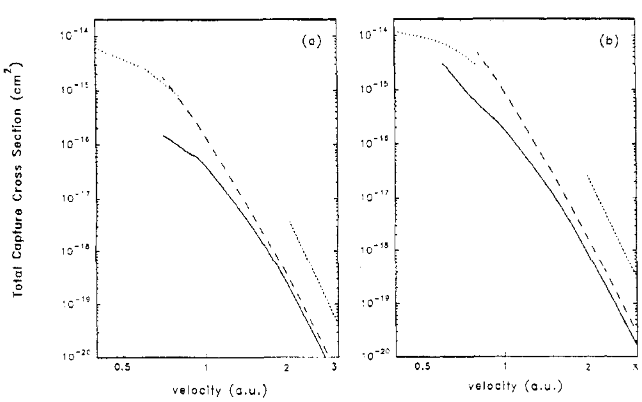

Fig. 2. Total capture cross section as a function of the impact velocity for protons (a) and alpha particles (b) colliding with H(2p). Notation as in Fig. 1.

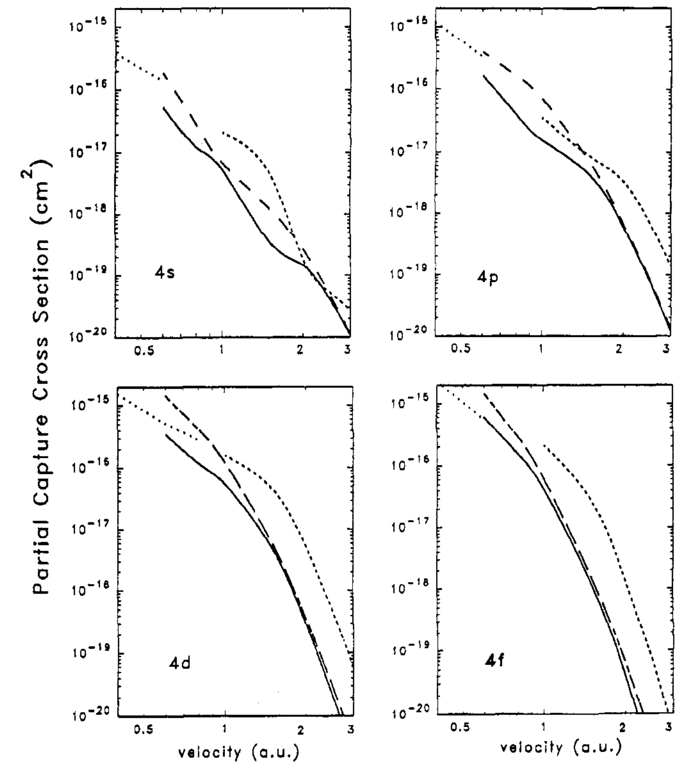

Fig. 3. Partial capture cross section to different $n_f = 4$ final states for collisions of He^{2+} projectiles on H(2s) as a function of the impact velocity. Notation as in Fig. 1.

which are probably related to the number of nodes of the radial final wave function. Such kinks do not leave any footprint at the level of the capture cross section to the shell $n_f = 4$, as shown in Fig. 5. They counterbalance each other when partial cross sections are added to give a smooth total cross section. Again, the EI and CDW cross sections

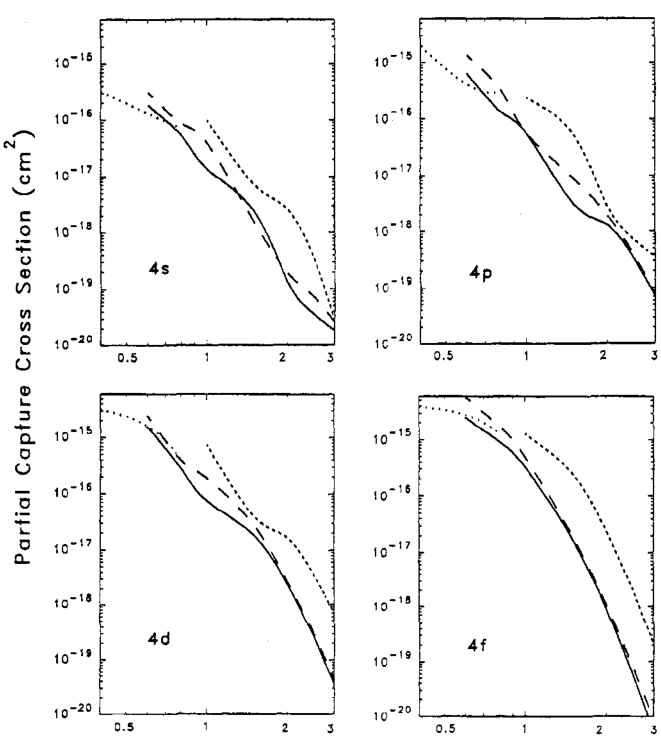

Fig. 4. Similar to Fig. 3 for Li^{3+} projectiles. Notation as in Fig. 1, except that dotted line now denotes the close-coupling calculations of Toshima and Lin [8].

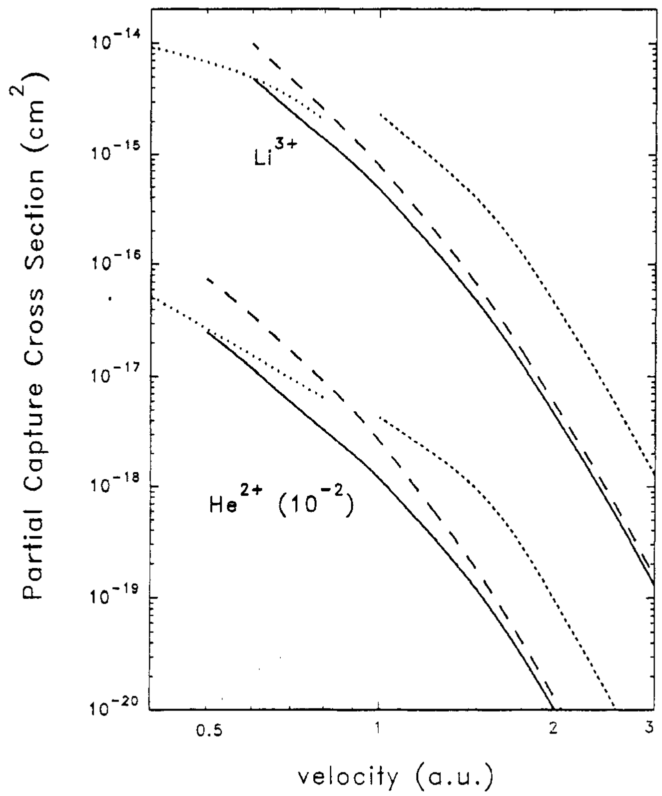

Fig. 5. Partial capture cross section into the final level $n_f = 4$ for collisions of He^{2+} and Li^{3+} ions on H(2s) as a function of the impact velocity. Notation as in Figs 3 and 4.

approach the CC results as the velocity decreases from below and above, respectively.

As it is usual in the performance of the CDW and EI methods, they tend to the same limit for high impact energies but for intermediate energies they become larger and smaller than the CC results, respectively. Before proceeding to the next section, one question should be answered: What method, the CDW approximation or the EI one, is the more reliable in the range of energies considered here? Since there are no available experiments, we are forced to compare both theoretical methods with the CC calculations of Lin and collaborators for the intermediate energies. However, from this comparison no definitive answer can be achieved because in most of the cases when a numerical agreement is found, the slopes are different. Certainly, for 2p – initial state the CDW approximation seems to have a better performance than the EI one as both methods are compared with CC values of Esry *et al.* [7]. A further question can be posed: Is the highest-energy extreme of the CC curves displayed in Figs 1–5 correct? If the atomic basis set is not complete enough, the CC calculations will tend to the BK1 values for high energies. It could explain the different crossing slopes between the CDW and CC curves.

3. Scaling rule

In Refs [11, 12] we derived scaling rules for partial capture cross sections by multicharged ions colliding with H(1s) and He(1s^2) in the high and intermediate energy region. A large amount of results was plotted in a comprehensible way using the proposed scaling. Although the scaling was obtained from the EI approximation, many other theoretical methods, including the CDW approximation, also verify it. In the present section we extend the scaling rule for capture from the initial level $n_i = 2$.

At intermediate and high impact energies, the EI capture cross sections from the initial state $i = n_i l_i m_i$ into a given n_f-level, $\sigma^{\mathrm{EI}}_{i,n_f}$, satisfy:

$$S^{\mathrm{EI}}_{i,n_f} = \frac{\tilde{z}_P^{7+2l_i}\sigma^{\mathrm{EI}}_{i,n_f}}{|C(Z_P/v)|^2} \simeq U_{Z_T,i,n_f}(\tilde{W}_{P_z}), \tag{1}$$

where

$$C(a) = \exp(\pi a/2)\Gamma(1 - \mathrm{i}a) \tag{2}$$

is the Coulomb factor coming from the asymptotic conditions. $U_{Z_T,i,n_f}(\tilde{W}_{P_z})$ denotes a universal function depending on the target charge Z_T (in our case $Z_T = 1$), on the initial state i and on the principal quantum number of the final shell n_f. The parameter $\tilde{W}_{P_z}$ is the scaled transfer momentum

$$\tilde{W}_{P_z} = \frac{W_{P_z}}{\tilde{z}_P} = \frac{\tilde{v}^2 + \tilde{z}_T^2 - 1}{2\tilde{v}}, \tag{3}$$

with W_{P_z} being the component of the usual transfer momentum of the projectile parallel to the incident velocity vector [15]. The scaled parameters (denoted with tildes) are defined as

$$\tilde{z}_P = \frac{Z_P}{n_f}, \quad \tilde{v} = \frac{v}{\tilde{z}_P}, \quad \tilde{z}_T = \frac{Z_T/n_i}{\tilde{z}_P}. \tag{4}$$

The only difference between eq. (1) and the one derived in Refs [11, 12] is the presence of $\tilde{z}_P^{7+2l_i}$ instead of $\tilde{z}_P^7$. This new expression allows us to consider capture from initial states with $l_i \neq 0$. In the derivation of eq. (1) fully stripped projectiles were considered, and the condition $\tilde{z}_T < 1$ was employed at intermediate velocities. Thence, the validity range of the proposed scaling is given by $\tilde{z}_T < 1$ in the intermediate and high energy region, and $\tilde{z}_T \geqslant 1$ in the high energy region.

In Fig. 6(a) we show the scaled cross section for capture from H(2s) to the final levels $n_f = 1 - 4$ by H^+, He^{2+}, and Li^{3+} projectiles, as a function of the scaled transfer momentum $\tilde{W}_{P_z}$. As it was observed for electron capture from the ground state [11], all the results corresponding to the 2s-initial state for different final shells can be gathered in a narrow strip, showing a smooth variation of the function $U_{Z_T,i,n_f}(\tilde{W}_{P_z})$ with n_f. Along with the EI results we plot in

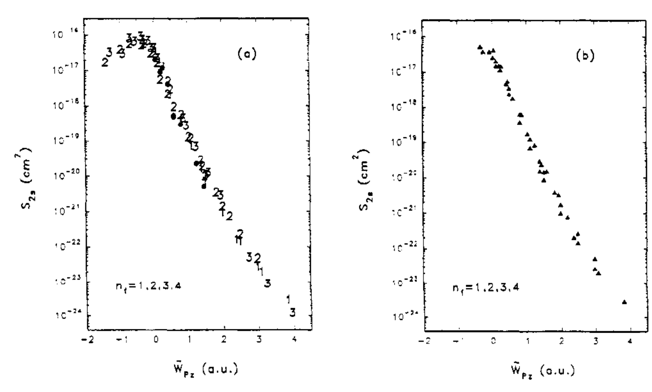

Fig. 6. Scaled partial cross section, S_{2s,n_f}, given by eq. (1) for capture from H(2s) to the final levels $n_f = 1 - 4$ as a function of $\tilde{W}_{P_z}$. (a) EI results (the numbers show the corresponding projectile charges Z_P); filled circles, CC calculations of Esry *et al.* [7] ($Z_P = 1$ with $n_f = 2$, 3 and $Z_P = 2$ with $n_f = 3$, 4) and Toshima and Lin [8] ($Z_P = 3$ with $n_f = 4$); (b) filled triangles, CDW results for $Z_P = 2$, 3.

Fig. 6(a) the CC results of Esry *et al.* [7] for capture to $n_f = 2,3$ by protons and to $n_f = 3,4$ by alpha particles, and those of Toshima and Lin [8] to $n_f = 4$ by Li^{3+} projectiles. In all the cases the velocities considered are 0.6 a.u. and 0.8 a.u. These CC results verify the scaling quite well, though the velocities considered by Esry *et al.* [7] for protons are out the validity range of our scaling.

In Figs 7(a) and 8(a) we show the scaled cross sections as given by eq. (1) for capture from the initial states $2p_0$ and $2p_1$ of hydrogen, respectively. In both cases, the EI results for final levels $n_f = 1 - 3$ of H^+, He^{2+}, and Li^{3+} projectiles can be enclosed within a thin strip as they are plotted as function of the scaled transfer momentum $\tilde{W}_{P_z}$. Note that in Figs 7 and 8, the EI results corresponding to the energy region $1 > \tilde{v} > \tilde{z}_T$ are not included because in this region the band corresponding to $n_f = 1$ escapes from the universal trend. *A priori* one does not have evidence to infer the dependence of $U_{Z_T,i,n_f}(\tilde{W}_{P_z})$ with n_f; the light variation with n_f observed for the initial states with $l_i = 0$ is an important finding, which may save a lot of computing time. It is also interesting to note that the values discarded (the ones satisfying $1 > \tilde{v} > \tilde{z}_T$) are precisely those that underestimate the results of Esry *et al.* [7] in Fig. 2. We also find that all the results fall within a relatively-thin strip if scaled cross sections of the initial states 2_0 and $2p_1$ are plotted together. This behavior show a weak dependency of the scaling curves with the initial magnetic quantum number m_i.

In Figs 6(b), 7(b) and 8(b) we show CDW results calculated by using the same scaling and for the same parameters as in Fig 6(a), 7(a) and 8(a), respectively. It can be observed that the CDW approximation verifies the proposed scaling,

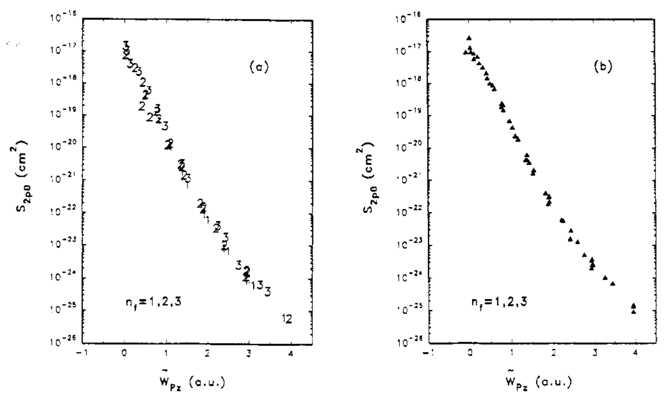

Fig. 7. Scaled partial cross section, S_{2p_0,n_f}, given by eq. (1) for capture from $H(2p_0)$ to the final levels $n_f = 1 - 3$ as a function of $\tilde{W}_{P_z}$. (a) EI results (the numbers show the corresponding projectile charges Z_P); (b) filled triangles, CDW results for $Z_P = 2, 3$.

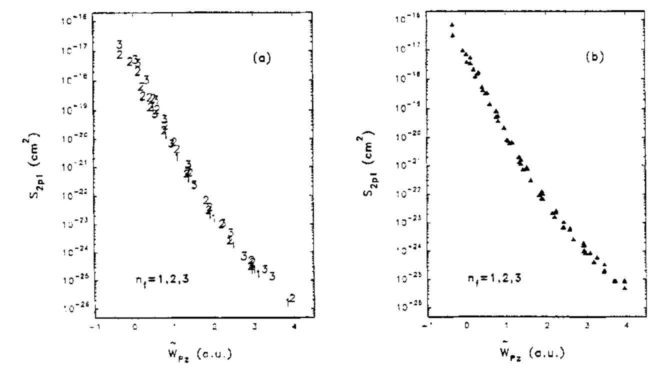

Fig. 8. Similar to Fig. 7 for capture from $H(2p_1)$.

even with less spread than the EI one. In all cases, the CDW universal curve is in good agreement with the EI one for $\tilde{W}_{P_z} \geqslant 0$, and they separate each other as $\tilde{W}_{P_z}$ becomes negative.

4. High-energies limits

In electron capture processes at very high impact energies it is widely recognized that the contribution from the BK2 cross section dominates the contribution from the BK1 one [16, 17]. The BK1 approximation only gives us a quick reference of the simplest approach, while the BK2 one provides the contribution of the double-scattering mechanism. A systematic study of the charge transfer process with BK1 and BK2 approximations was published by Briggs and Dubé [18, 19] some years ago. These authors investigated the capture from 1*s*-state to different final states. In this Section we extend their study for capture from $n_i = 2$.

We study the asymptotic forms of BK1 and BK2 cross sections, $\hat{\sigma}_{i,f}^{BK1}$ and $\hat{\sigma}_{i,f}^{BK2}$, respectively, for high but non-relativistic velocities. The asymptotic forms $\hat{\sigma}_{i,f}^{BK1}$ and $\hat{\sigma}_{i,f}^{BK2}$ have the following expressions:

$$\hat{\sigma}_{i,f}^{BK1} = A_{i,f} \frac{Z_T^{5+2l_i} Z_P^{5+2l_f}}{v^{12+2l_i+2l_f}} \pi, \tag{5}$$

and

$$\hat{\sigma}_{i,f}^{BK2} = \frac{B_{n_i l_i, n_f l_f}}{v^{11}} \mid Y_{l_i}^{m_i}(60°) \mid^2 \mid Y_{l_f}^{m_f}(60°) \mid^2. \tag{6}$$

The coefficient $A_{i,f}$ has a close-form, depending only on the initial and final quantum numbers, $n_i l_i m_i$ and $n_f l_f m_f$, respectively. The coefficient $B_{n_i l_i, n_f l_f}$ depends on the quantum numbers n_i, l_i, n_f, l_f, and on Z_T and Z_P. The angle of 60° appearing in the Spherical Harmonics in eq. (6) is according to the classical description of the double-scattering process given by Thomas [16]. In this description the electron scatters off the projectile ion through 60° with respect to the beam direction, and then through 60° off the target nucleus in such a way as to leave the electron with almost zero momentum with respect to the projectile nucleus. The relation between the classical and the quantum descriptions of this mechanism was set up by Shakeshaft [20]. Some values of $A_{i,f}$ and $B_{n_i l_i, n_f l_f}$ of interest here are listed in Tables I and II, respectively.

The asymptotic forms $\hat{\sigma}_{i,f}^{BK1}$ and $\hat{\sigma}_{i,f}^{BK2}$ allow us to estimate the energy where Thomas mechanism starts being domi-

Table I. *Coefficients $A_{i,f}$ (in a.u.) corresponding to the asymptotic form of BK1 capture cross section given by eq. (5)*

	Initial states			
Final states	1s	2s	$2p_0$	$2p_1$
1s	5.24 (+4)	6.55 (+3)	1.87 (+4)	1.56 (+3)
2s	6.55 (+3)	8.19 (+2)	2.34 (+3)	1.95 (+2)
$2p_0$	1.87 (+4)	2.34 (+3)	7.28 (+3)	4.55 (+2)
$2p_{\pm1}$	1.56 (+3)	1.95 (+2)	4.55 (+2)	6.50 (+1)
3s	1.94 (+3)	2.43 (+2)	6.93 (+2)	5.78 (+1)
$3p_0$	6.58 (+3)	8.22 (+2)	2.56 (+3)	1.60 (+2)
$3p_{\pm1}$	5.48 (+2)	6.85 (+1)	1.60 (+2)	2.28 (+1)
$3d_0$	2.68 (+3)	3.35 (+2)	1.12 (+3)	4.95 (+1)
$3d_{\pm1}$	5.68 (+2)	7.10 (+1)	1.86 (+2)	2.07 (+1)
$3d_{\pm2}$	4.06 (+1)	5.07 (+0)	1.03 (+1)	1.94 (+0)

Table II. *Coefficients $B_{n_i l_i, n_f l_f}$ (in a.u.) corresponding to the asymptotic form of BK2 capture cross section given by eq. (6)*

Final states	Initial states 1s	2s	2p
1s	9.97 (+4)	1.20 (+4)	3.08 (+2)
2s	1.20 (+4)	1.85 (+3)	3.25 (+1)
2p	3.08 (+2)	3.25 (+1)	3.25 (+1)
3s	3.65 (+3)	6.70 (+2)	1.97 (+1)
3p	1.03 (+2)	2.40 (+1)	8.51 (+0)
3d	1.44 (+0)	1.32 (+0)	1.70 (+0)

nant. By using eqs (5) and (6) we calculate the crossing velocity, v_c, at which the v^{-11} term corresponding to $\hat{\sigma}_{i,f}^{\mathrm{BK2}}$ becomes bigger than the $v^{-12-2l_i-2l_f}$ term corresponding to $\hat{\sigma}_{i,f}^{\mathrm{BK1}}$; namely

$$\hat{\sigma}_{i,f}^{\mathrm{BK1}}(c_c) = \hat{\sigma}_{i,f}^{\mathrm{BK2}}(v_c). \quad (7)$$

For capture from the ground state Dubé and Briggs [19] found that the larger l_f, the smaller v_c. The relative importance of the double scattering is emphasized for capture from $n_i = 2$. We find that v_c falls down drastically when l_f is increased. For example, for proton on hydrogen collisions the transition $2p_1 \to 1s$ gives $v_c = 15.8$ [19], while the transition $2p_1 \to 2p_1$ gives $v_c = 3.8$ and $2p_1 \to 3d_2$, $v_c = 2.4$. Note that velocities where the second Born approximation strongly contributes are included in the high-energy extreme of our range of interest. On the other hand, if the CC calculations were extended to velocities $v \sim v_c$, the intermediate states that contribute decisively to $\hat{\sigma}_{i,f}^{\mathrm{BK2}}$ (namely the continuum) should be properly described, so the basis set of work might be quite large.

It is known for years that the BK1 cross section contains the appropriate parametric dependence, even though its absolute value is quite large, as it is observed in Figs 1–5. We can easily prove that the asymptotic form $\hat{\sigma}_{i,f}^{\mathrm{BK1}}$ satisfies the scaling rule proposed. For large velocities $\tilde{W}_{Pz} = W_{Pz}/\tilde{z}_P \sim (v/2)/\tilde{z}_P$ and $C(Z_P/v) \sim 1$. Then we can rewrite eq. (5) as

$$\hat{\sigma}_{i,f}^{\mathrm{BK1}} = \tilde{z}_{P-7-2l_i} U_{ZT,i,n_f}^{\mathrm{BK1}}(\tilde{W}_{Pz}), \quad (7)$$

which is precisely the scaling rule discussed in Section 3.

5. Conclusions

We have calculated total and partial capture cross sections from excited states H(2s) and H(2p) by collisions with H^+, He^{2+} and Li^{3+} ions, by using the EI and CDW approximations at moderate and high impact velocities. After comparing these results with other theoretical values and with the highest-energy extreme of existing close-coupling calculations, we conclude that for capture from H(2s) the EI and CDW approximations produce acceptable performances. For total capture from H(2p) the EI approximation seems to give small values at intermediate energies if compared with the CC and CDW calculations. Beside this theoretical contrast, experimental data should be desirable to extract definitive conclusions.

We have also proposed a scaling rule in terms of the projectile charge for the partial cross sections. It allows us to plot results for different projectiles and final levels on a universal band. This rule is not only satisfied by the EI values but also by the CDW and CC calculations.

Finally, we have estimated the relative importance of the double scattering over the single scattering mechanism for capture from $n_i = 2$. We have found that the double mechanism contributes drastically for the highest velocities considered in this work.

Acknowledgements

We like to thank to Prof. R. D. Piacentini for illuminating discussions on the subject.

References

1. Summers, H. P., in: "Advances in Atomic, Molecular and Optical Physics" (Edited by M. Inokuti) (New York, Academic Press 1994), Vol. 33, p. 275.
2. Gilbody, H. B., in: "Proceedings of XIX International Conference on The Physics of Electronic and Atomic Collisions" (Edited by L. J. Dubé, J. B. A. Mitchell, J. W. McConkey, and C. E. Brion) (AIP Press, New York 1995), p. 19.
3. Salop, A., Phys. Rev. **A13**, 1321 (1976).
4. Casaubon, J. I. and Piacentini, R. D., J. Phys. **B17**, 1623 (1984).
5. Blanco, S. A., Falcón, C. A., Reinhold, C. O. and Piacentini, R. D., J. Phys. **B19**, 3945 (1986).
6. Blanco, S. A., Falcón, C. A., Reinhold, C. O., Casaubon, J. I. and Piacentini, R. D., J. Phys. **B20**, 6295 (1987).
7. Esry, B. D., Chen, Z., Lin, C. D. and Piacentini, R. D., J. Phys. **B26**, 1579 (1993).
8. Toshima, N. and Lin, C. D., Phys. Rev. **A47**, 4831 (1993).
9. Chan, F. T. and Eichler, J., J. Phys. **B12**, L305 (1979).
10. Gravielle, M. S. and Miraglia, J. E., Phys. Rev. **A44**, 7299 (1991).
11. Gravielle, M. S. and Miraglia, J. E., Phys. Rev. **A51**, 2131 (1995).
12. Gravielle, M. S. and Miraglia, J. E., Phys. Rev. **A52**, 851 (1995).
13. Belkić, Dz., Gayet, R. and Salin, A., Phys. Rep. **56**, 279 (1979).
14. Jouin, H. and Harel, C., J. Phys. **B24**, 3219 (1991).
15. $\mathbf{W}_P = \mathbf{K}_i - \mu_P \mathbf{K}_f$, with $\mu_P = M_P/(M_P + 1)$ in the usual notation.
16. Thomas, L. H., Proc. R. Soc. **A114**, 561 (1927).
17. Shakeshaft, R. and Spruch, L., Rev. Mod. Phys **51**, 369 (1979).
18. Briggs, J. S. and Dubé, L. J., J. Phys. **B13**, 771 (1980).
19. Dubé, L. J. and Briggs, J. S., J. Phys. **B14**, 4595 (1981).
20. Shakeshaft, R., J. Phys. **B7**, 1059 (1974).